Mutagenesis vol. 24 no. 2 pp. 191–197, 2009
Advance Access Publication 12 January 2009
doi:10.1093/mutage/gen071

A direct view by immunofluorescent comet assay (IFCA) of DNA damage induced by nicking and cutting enzymes, ionizing ^{137}Cs radiation, UV-A laser microbeam irradiation and the radiomimetic drug bleomycin

Paulius Grigaravičius[1,*], Alexander Rapp[1,2] and Karl Otto Greulich[1]

[1]Leibniz Institute for Age Research—Fritz Lipmann Institute, Beutenbergstrasse 11, D-07745 Jena, Germany

In DNA repair research, DNA damage is induced by different agents, depending on the technical facilities of the investigating researchers. A quantitative comparison of different investigations is therefore often difficult. By using a modified variant of the neutral comet assay, where the histone H1 is detected by immunofluorescence [immunofluorescent comet assay (IFCA)], we achieve previously unprecedented resolution in the detection of fragmented chromatin and show that trillions of ultraviolet A photons (of a few eV), billions of bleomycin (BLM) molecules and thousands of γ quanta (of 662 keV) generate, in first order, similar damage in the chromatin of HeLa cells. A somewhat more detailed inspection shows that the damage caused by 20 Gy ionizing radiation and by a single laser pulse of 10 μJ are comparable, while the damage caused by 12 μg/ml BLM depends highly on the individual cell. Taken together, this work provides a detailed view of DNA fragmentation induced by different treatments and allows comparing them to some extent, especially with respect to the neutral comet assay.

Introduction

In DNA double-strand break (DSB) repair studies, a standardized tool for inducing DNA damage is not available. Different DNA damaging treatments or agents are applied. An affordable approach is the use of radiomimetic drugs such as bleomycin (BLM) (1). Visible or ultraviolet (UV) radiation is used by those who are interested in repair of damage caused by sunlight, whereas those interested in radiation therapy use ionizing radiation. Additionally, in the last decade, an interest in using laser microbeams has increased (2–4). Focused laser radiation allows very precise microprocessing of single cells, nuclei, organelles and parts of chromosomes (5,6) and thus can induce highly localized DNA damage with high temporal resolution (2–4).

The level of induced DSBs primarily can be estimated from the dose of applied agents, although dose definitions for each of the damaging agents are different. Grays (Gy) are used for ionizing irradiation, concentration (μg/ml) for biochemical damaging like drugs or enzymes and Joules (J) for UV and visible light. Consequently, they cannot be compared directly. This lack of comparability of DNA fragmentation induced by different agents has a consequence that the synergies in the knowledge on DNA damage and subsequent repair are presently not optimally used. Thus, in this work, we compare directly and quantitatively doses of ionizing radiation (^{137}Cs), a UV-A laser microbeam (349 nm) and BLM that induce similar DNA fragmentation levels in HeLa cells. We still have to keep in mind that the above-mentioned agents induce also single-strand breaks (SSBs). DSB/SSB induction ratios are about 1:20 for ionizing irradiation (7) and 1:6–10 for BLM (8,9). UV-A mainly induces SSBs, but depending on the energy density can generate DSBs although the ratio is not yet known. Due to the fact that SSB alone does not generate fragments, we assume that fragmentation is caused by DSBs.

For the detection of DNA fragmentation at the single-cell level, we present and use a novel version of the neutral comet assay. It is widely believed that the conventional neutral comet assay, in which lysis and electrophoresis are carried out at pH 8, detects DNA strand breaks (10,11), but whether it detects solely DSBs or also SSBs is still under discussion (12). However, the common DNA dye-based staining techniques used in previous approaches provide only limited resolution of the comets. Thus, visualization of details is not possible and the subtle differences in neutral comets after various treatments are not revealed.

Here, we introduce and apply a staining method using antibodies [immunofluorescent comet assay (IFCA)] against histone H1. This enables direct visualization with high resolution of fragmented chromatin, exploiting the fact that the linker histone H1 is tightly bound to the DNA. It has already been reported in the literature that even after proteinase treatment some proteins still remain bound to DNA in the comet assay (13,14). In the present work, we show that histone H1 is still bound to DNA after electrophoresis and can be detected by immunofluorescence staining. Using this technique, we provide a detailed look into the neutral version of the comet assay at high resolution and even give an estimate for the size of fragments at the end of the comet tail.

Materials and methods

Cell culture

HeLa cells were maintained in RPMI medium containing 10% foetal calf serum (FCS), 10 000 U/l penicillin and 100 mg/l streptomycin at 37°C, 5% CO_2. Two days before the experiments, cells were seeded into 3.5-cm culture dishes.

Comet assay

The comet assay was performed immediately after the DNA damage was induced as described earlier (11,15) to avoid DNA repair. Briefly, cells were washed with phosphate-buffered saline (PBS), trypsinized and suspended in medium with FCS to block the trypsin activity. Subsequently, cells were centrifuged for 10 min at 2000× *g*. After removal of the medium, the cells were washed with PBS, centrifuged again, re-suspended in PBS and diluted 1:4 with 1% agarose in PBS. In all, 100 μl of the cell suspension in 0.8% agarose was added on the pre-warmed fully frosted slides with middle layer and sealed with a coverslip. After lysis [0.5% sodium dodecyl sulphate (SDS) and 33 mM ethylenediaminetetraacetic acid (EDTA)] at room temperature for 40 min, the slides were incubated for 10 min in 1× Tris/Borate/EDTA (TBE) buffer (89 mM

*To whom correspondence should be addressed. Tel: +49 3641 656409; Fax: +49 3641 656410; Email: paulius@fli-leibniz.de
[2]Present address: Department of Biology, Technische Universitaet Darmstadt, Schnittspahnstrasse 10, D-64287 Darmstadt, Germany

Tris, 89 mM boric acid and 0.2 mM EDTA, pH 8.3) and electrophoresed in 1× TBE buffer at 1 V/cm for different times, as indicated in the Results. For the alkaline comet assay, slides were incubated in alkaline lysis buffer (2.5 M NaCl, 0.1 M EDTA, 10 mM Tris-base, 0.2 M NaOH, 1% SDS, 1% Triton and 10% dimethyl sulphoxide) for 60 min at 4°C. Subsequently, they were placed in electrophoresis buffer (0.3 M NaOH and 1 mM EDTA, pH > 13) for 25 min in order to unwind the DNA and electrophoresed at 1 V/cm for 25 min or 2 h, after electrophoresis slides were neutralized in Tris buffer (0.4 M Tris–HCl, pH 7.5) for 5 min.

Lambda DNA (48.5 kbp) migration in neutral comet assay

Frosted slides with two windows (Erie Scientific Company, Portsmouth, USA) were covered with 400 µl of 0.8% low-melting point agarose in PBS, sealed with coverslip and cooled down. After 10 min of incubation in an electrophoresis tank with 1× TBE buffer, the 25 µg/ml lambda DNA (New England Lab, Ipswich, USA) diluted in PBS was added by the following. With the top of the 10-µl tip, a small pocket was formed in agarose layer (as shown in Figure 2G) and ~0.2 µl of 1:1 lambda DNA and DNA loading dye mixture was loaded. After 25 min of electrophoresis, 30 µl of antifade solution containing YOYO1 or SYBR Green was added to the slides and sealed with a coverslip. A slightly different procedure was done for electrophoresing the low-range pulsed field gel electrophoresis (PFGE) marker purchased from New England Lab. The marker DNA is delivered in 1% agarose, thus it was cut into small pieces with diameter of ~500 µm. These pieces were attached to the frosted slide with two windows and covered with 400 µl of 0.8% low-melting point agarose in PBS. Consequently, the slides were covered with a cover glass and cooled down. Further processing was done as described above.

Immunofluorescent comet assay

After single-cell gel electrophoresis, the slides were washed in PBS, followed by the addition of mouse monoclonal anti-histone H1 antibody (AE-4, Santa Cruz Biotechnology, Santa Cruz, USA) diluted 1:50 in 60 µl of PBS/7% bovine serum albumin (BSA) and sealed with a plastic coverslip. Incubation was performed in a humid chamber overnight. Next day, the slides were washed in PBS, PBS with 0.05% Tween-20 and PBS for 15 min each and incubated with secondary donkey anti-mouse antibody conjugated with Alexa 488 or Alexa 594 fluorescent dyes (dilution 1:400 in PBS/7% BSA, Invitrogen, Karlsruhe, Germany). After 1.5 h of incubation, the slides were washed again as described above and mounted in 4′,6-diamidino-2-phenylindole (DAPI)/antifade [1 µg/ml DAPI, 100 mM DABCO, 45% glycerol and 10 mM Tris–HCl (pH 8.0)] or for colocalization experiments, slides were embedded in 1 µM SYBR Green in antifade solution and finally sealed with a coverslip.

Enzymatic induction of DNA fragmentation

For generation of defined numbers of SSBs and DSBs, we used the nicking and restriction endonucleases Nt.BbvCI and BbvCI, respectively (New England Lab). Both enzymes recognize the sequence 5′-CCTCAGC, but induce either a SSB (nick) (Nt.BbvCI) or a DSB (BbvCI). Untreated HeLa cells were embedded in microgels, lysed in neutral lysis buffer as described above and subsequently washed once in TE (10 mM Tris and 1 mM EDTA, pH 8) buffer for 10 min, then twice for 15 min in 1× restriction reaction buffer (NEB buffer 4: 50 mM potassium acetate, 20 mM Tris acetate, 10 mM magnesium acetate, 1 mM dithiothreitol, pH 7.9). Subsequently, 15 units of the enzyme diluted in 100 µl of the 1× restriction reaction buffer were added to the slides. One unit is the amount of Nt.BbvCI enzyme required to convert 1 µg of supercoiled plasmid DNA to open circular form in 1 h at 37°C in a total reaction volume of 50 µl. For BbvCI, one unit is defined as the amount of enzyme required to digest 1 µg of lambda DNA at the same conditions. The slides were covered with a plastic coverslip and incubated at 37°C in a humid chamber for 3 h, washed with PBS for 15 min, incubated in 1× TBE and electrophoresed as described above.

Damage induction and quantitative calculation of used photons, doses and molecule numbers by ionizing radiation, UV-A laser microbeam irradiation and BLM treatment

With the assumption that the size of a HeLa cell nucleus is $10 \times 10 \times 3\ \mu m^3$, it will have a volume of 300 μm^3 or 300 fl. The weight of such cell nucleus will be 300 pg (assuming a density of 1 g/ml).

Ionizing radiation. γ Irradiation was performed using a Gammacell GC40 with ^{137}Cs (Nordion, Ottawa, Canada). Doses were defined via the time of exposure (dose rate: 1.17 Gy/min) of the γ source. Since 1 Gy is strictly a dose absorbed by the tissue and not the dose emitted by the γ source, one has to assume that the biological material absorbs the ionizing radiation like water. This assumption is in agreement with the medical literature.

The ionizing irradiation dose is defined as the absorbed energy per 1 kg of biological tissue, thus 1 Gy = 1 J/kg = 10^{-3} J/g. In this case, one cell nucleus will absorb 0.3 pJ (10^{-3} J/g × 300 × 10^{-12} g = 300 × 10^{-15} J = 0.3 pJ). This energy is an equivalent for (0.3 × 10^{-12} J)/(1.6 × 10^{-19} J/eV) = 1.5 × 10^6 eV. One γ photon of ^{137}Cs has an energy of 662 keV. Thus, one single-cell nucleus formally absorbs the whole energy of (1.55 × 10^6 eV)/(662 000 eV) = 2.3 γ photons. However, a 3-µm thick nucleus is not able to absorb the whole energy of one photon because the linear energy transfer (LET) of γ photons is 0.8 keV/µm. Thus, we will need 625 γ photons with 0.8 keV LET in order to apply 1-Gy irradiation dose on one single nucleus.

Laser microbeam. Laser microirradiation was performed by a pulsed UV-A laser microbeam (frequency tripled Nd:YLF laser generating ~20 ns pulses at 349 nm from Spectra Physics, Mountain View, USA) coupled via the epifluorescence illumination path into a confocal laser scanning microscope (LSM 510, Zeiss, Jena, Germany) (16).

The pulse energy used to irradiate the single-cell nucleus was ~10 µJ in the optical plane of sample. In the following, we will convert the absorbed dose into an equivalent for ionizing radiation (J/kg) and will find out how many photons this irradiation needs for induction of DSBs. The penetration depth of such wavelength in biological tissue is ~60 µm (5). By using the Lambert–Beer law, the pulse in the depth of 3 µm will have the energy $I_{3\ \mu m} = I_0 e^{-dl}$: $I_{3\ \mu m} = I_0 e^{-3/60} = 0.95\ I_0$ from here the absorbed energy is $I_A = 0.05\ I_0 = 0.5$ µJ or 3.13 × 10^{12} eV. A single photon at 349 nm has an energy of 3.5 eV, thus the cell nucleus absorbs ~1 × 10^{12} photons. Here, we have to note that in the case of laser microbeam, the energy is absorbed locally only in the irradiated region with a volume of 3 μm^3 (for a 3-µm thick nucleus) or 3 pg. From these numbers, we can calculate the absorbed energy per mass unit: (0.5 × 10^6 J)/3 × 10^{-12} g = 0.5/3 × 10^{-6} J/g = 0.17 × 10^9 J/kg. This is a dimension of Gy that is usually used only for ionizing radiation.

Bleomycin. For BLM damage, we added the BLM (Biomol, Hamburg, Germany) to the medium to a final concentration of 12 µg/ml. The cells were then incubated at standard conditions for 30 min.

The molecular weight of BLM is 1415 g/mol. Thus, the molarity in the cell nucleus is 8.5 µM, if we assume that BLM is equally distributed in the solution and the cell, this represents 5.12 × 10^{18} molecules in 1 litre. With a volume of the cell nucleus of 300 fl, the number of BLM molecules in the single-cell nucleus will be (5.12 × 10^{18} molecules/litre) × (0.3×10^{-12} litre) = 1.5 × 10^6 molecules.

All important parameters of different treatments are summarized in Table I.

Microscopy and image analysis

Imaging of the samples was performed using a microscope with structured illumination for quasi-confocal microscopy. The Apotome unit (Zeiss) is mounted into the epifluorescence illumination path of an Axiovert 200 (Zeiss). Filtersets for DAPI (Zeiss No 49), FITC (Zeiss No 38 HE) and Cy3 (Zeiss No 43 HE) were used. The camera (Zeiss, MRM Axiocam) as well as the structured illumination were controlled by Axiovision software (Zeiss). Macro imaging of ~1 cm^2 was performed using a Zeiss laser scanning microscope (LSM 510) equipped with a HeNe and an Argon ion lasers and emission filterset for the detection of FITC (BP530/20) as well as for rhodamine signals (LP 580, LP 625).

In silico sequence analysis

In silico restriction fragmentation analysis for fragmentation of the whole human genome by cutting enzyme BbvCI was done by using Clone manager (for sequence manipulation and analysis) and OriginPro (for data analysis and graphical representation) software. *In silico* calculation of the number of potential DSBs arising due to closely spaced SSBs by the nicking enzyme Nt.BbvCI was done only for chromosome 6. Sequences of all human

Table I. Comparison of important parameters for every type of treatment

Treatment	Photon energy	Dose	Absorbed energy	Number of photons needed	Molecules per nucleus
20 Gy (137Cs)	661 keV	20 Gy or J/kg	0.6 × 10^{-12} J	12.5 × 10^3	
10 µJ UV-A, 350 nm laser pulse	3.5 eV	17 × 10^7 J/kg	1 × 10^{-6} J	1 × 10^{12}	
BLM 12 µg/ml					1.5 × 10^6

chromosomes were obtained from the website of National Center for Biotechnology Information (http://www.ncbi.nlm.nih.gov/).

Results

IFCA versus conventional SYBR Green staining

It is widely accepted that histone H1 is a protein strongly binding to DNA. Here, we show that it can be detected by immunofluorescence even after lysis and electrophoresis in the neutral comet assay. The possibility of using antibody staining of histone H1 enables the visualization of neutral comets with higher resolution or more detail than after the conventional DNA staining with SYBR Green.

Figure 1 directly compares conventional SYBR Green staining and IFCA for the neutral comet assay. The samples were double stained by both methods. The left column of Figure 1 shows images taken using a FITC filterset (SYBR Green). The right column shows images of the identical cells taken with a Cy3 filterset (IFCA). During image acquisition, care was taken not to overexpose the images and subsequently the images were processed identically in order to ensure a valid comparison. Additionally, the intensity profiles of the comets are shown (Figure 1E and F). With the conventional comet assay (left column, Figure 1A and C), at most faint tails are visible. In contrast, IFCA of the same cells reveals much more detail. Long single filaments emanate from the head. They can be recognized even in the untreated cell (Figure 1B), although this might be due to the intrinsic damage or due to experimental procedures. In the cells irradiated with 10 Gy (^{137}Cs, photon energy 662 keV), additional filaments emanate from the head as is evident from the intensity increase in the middle part of the tail from IFCA intensity profile comparison (Figure 1F, arrow). The small intensity increase at the end of the tail is due to the short fragments (Figure 1D), which are detected only by IFCA. A magnified view of this region marked with a frame in Figure 1D is additionally shown in Figure 1H.

An attempt to visualize these details with SYBR Green staining would require over exposure or crude processing of the images by increasing brightness and contrast. This was done in Figure 1G, where the SYBR Green and the IFCA signal colocalization is shown. Green represents DNA staining by SYBR Green whereas red is IFCA detection of histone H1. The image was processed in order to show the colocalization of signals especially at the end of the tail (insert in Figure 1G, top right). Yellow and orange (insert in Figure 1G) show that the signals in the neutral comet assay indeed do colocalize. This proves that histone H1 is still bound to DNA after lysis and electrophoresis, and IFCA truly visualizes chromatin.

Interestingly, we could detect a histone H1 signal by using IFCA even after the harsh conditions used in alkaline lysis and electrophoresis. Representative images of untreated and irradiated (10 Gy) HeLa cells after alkaline comet assay and IFCA staining are shown in Figure 1I and J, respectively. It shows that immunofluorescent staining of histone H1 reveals high level of details in the tails of both neutral and alkaline comets.

SSBs in neutral comet assay and fragment size estimation

In the following, we will elucidate the damaging mechanism by using the DNA-nicking enzyme Nt.BbvCI and the cutting restriction enzyme BbvCI with the same recognition site.

According to the literature, closely located SSBs within 14 nucleotides on opposite strands make the DNA structure unstable and they can be converted into DSBs at 37°C (17). Detailed *in silico* sequence analysis of chromosome 6 shows

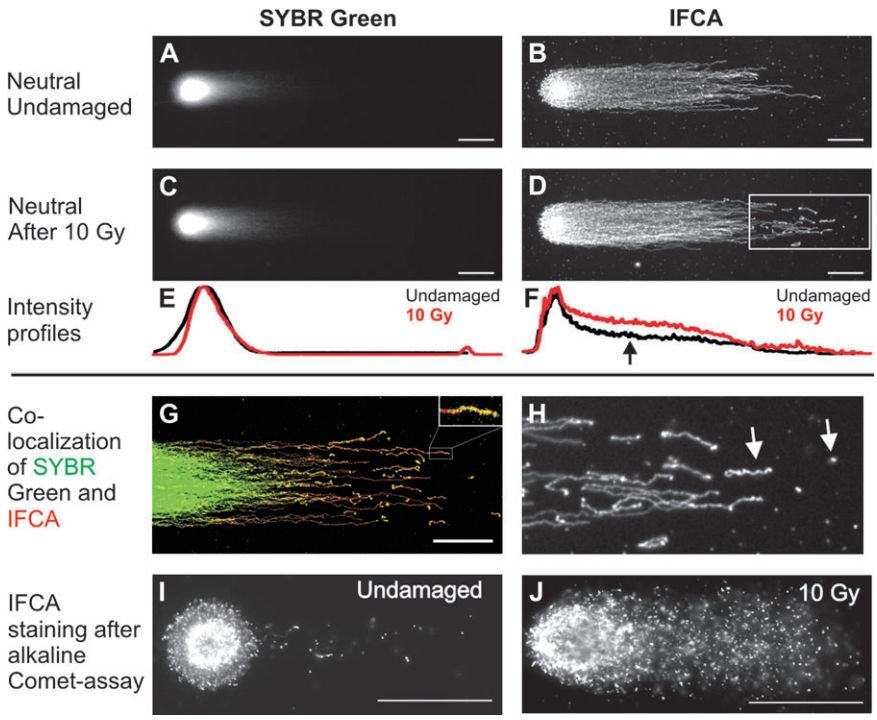

Fig. 1. Direct comparison of IFCA and SYBR Green staining for the neutral comet assay. (**A** and **C**) SYBR Green staining of the untreated cells (**A**) and cells after 10-Gy irradiation (**C**), intensity profiles of the same cells is shown in panel (**E**). (**B** and **D**) IFCA staining of neutral comet assay of the untreated (**B**) and with 10-Gy irradiated cells (**D**) where (**F**) represents intensity profiles. (**H**) Magnification of comet tail in (**D**) showing small dot-like and fibre-like fragments marked with arrows. (**G**) Colocalization of SYBR Green (green) and histone H1 (red) signals. IFCA signal completely colocalizes with SYBR Green. (**I** and **J**) IFCA staining after the alkaline comet assay untreated (**I**) and irradiated (**J**) with 10-Gy cells. Scale bars, 50 μm.

that Nt.BbvCI (nicking) can produce 49 pairs of SSBs that fulfil the requirements mentioned above. This means that theoretically 49 DSBs and 50 fragments due to clustered SSBs can be generated. Chromosome 6 contains ∼2.75% of whole human diploid genome sequence. Extrapolating this to the whole genome of a diploid cells, we would expect to have ∼1764 DSBs generated by clustered SSBs; this is equivalent to 44 Gy if 1 Gy of γ irradiation induces ∼40 DSBs per cell (18). In contrast, after BbvCI digestion (pure DSB induction), we would expect to obtain $\sim 2.8 \times 10^6$ DSBs and the same number of fragments (according to the whole genome *in silico* fragmentation analysis). Consequently, the comets and their profile intensities representing nicking (Figure 2B) and cutting (Figure 2C) show very large differences in the tails and no fragmentation is detected if cells are treated only with the buffer (Figure 2A). Figure 2B and E shows a number of fragments as a result of the action of the nicking enzyme Nt.BbvCI and thus represents SSBs converted to DSBs. In contrast, after the digestion with BbvCI, only a few fibres are still bound to the former nucleus (head) (Figure 2C and F, frame I). The majority of the genome is highly fragmented as predicted and is visible as a cloud of small fragments (Figure 2C and F, frame III). An even better insight into the fragmentation pattern can be obtained by extending the electrophoresis time up to 3 h (Figure 2E and F).

The damaging pattern after BbvCI treatment shows three different types of fragments. Figure 2F, frame I shows several long fibres emanating from the former nucleus (head), which

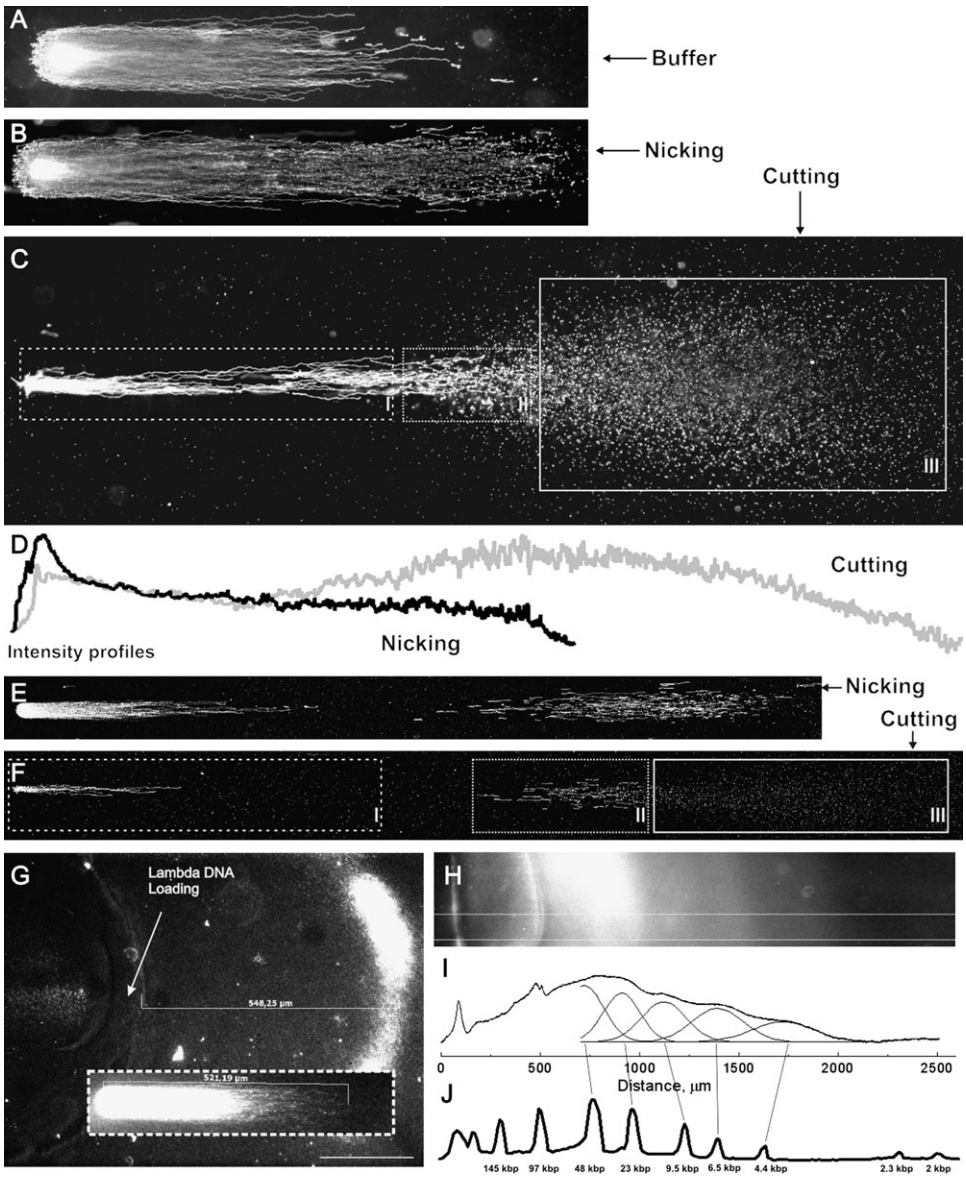

Fig. 2. SSBs and DSBs in the neutral comet assay. (**A**, **B** and **C**) Representative IFCA images of cells treated with enzyme buffer NEB4 as control (**A**), nicking Nt.BbvCI (**B**) and with cutting BbvCI (**C**) enzymes recognizing the same DNA sequence and electrophoresed for 25 min. (**D**) Intensity profiles. (**E** and **F**) Comets after the same treatment but 3 h of electrophoresis. (**G**) In the single-cell gel electrophoresis for 25 min, lambda DNA (48.5 kbp) migrate 530 µm, it means that fragments of such size are located at the end of the comet tail (neutral comet stained with YOYO1 is shown in the insert). (**H**) Migration of low-range PFGE marker in 25 min of neutral electrophoresis stained with SYBR Green. (**I**) Intensity profile of insert in (**H**) with the intensity profile modulation by using 5 Gaussian peak functions representing the distinct fragment sizes in PFGE (**J**). Neutral comet assay shows fragmentation of DNA after nicking enzyme treatment due to SSBs located in opposite strands close to each other (<14 nucleotides). After cutting with BbvCI, dot-like fragments in the size up to ∼50 kbp form a big cloud at the end of the comet tail (frame III).

are still connected to it. Frame II shows several tens of shorter but still stretched fibre fragments. The majority of signal in Figure 2C and F is dot like and forms a big cloud at the end of the comet tail (frame III). Interestingly, a detailed analysis of all human chromosome fragmentation by the BbvCI enzyme showed that almost all fragments (>99.9%) should be in the range from 5 bp to 30 kbp. Thus, we claim that fragments with the size up to 30 kbp migrate very fast and form a big cloud of dot-like fragments at the end of the tail (frame III). Additionally, we studied how DNA molecules of similar size migrate under the same conditions. We used lambda DNA with the size of 48.5 kbp. Figure 2G shows that after 25 min of electrophoresis, the 48.5 kbp sized DNA has migrated ~540 μm from the loading pocket and are found to be located at the end of the neutral comet tail (comet tail length in insert—520 μm). The 48.5-kbp DNA is not forming short stretched fibres but forms a dot-like structure (data not shown). This confirms that dot-like fragments in IFCA are up to 50 kbp. Longer fibres (frames I and II in Figure 2C) may occur because of incomplete restriction due to hardly accessible DNA. We cannot determine the highly interesting issue of whether those long fibres connected to the head in undamaged, as well as in damaged cells are stretched loops or chromosome ends.

Furthermore, Figure 2H shows the result of low-range PFGE marker electrophoresis done under the same conditions. The intensity profile of it was modulated by 5 Gaussian peaks representing fragments of distinct size (Figure 2I and J). This indicates that also fragments even down to 4.4 kbp are not washed away but are partially separated and can be detected in the neutral comet assay if a highly sensitive approach is used. Fragments with the size higher than 48 kbp are not well separated first due to the fact that the conventional gel electrophoresis in general cannot separate fragments larger than ~50 kbp and second because the introduced low-range PFGE marker gel piece diameter is ~500 μm. It means that the peaks representing high-molecular weight molecules (143—50 kbp) after short migration are very broad and are located within 500 μm from the marker gel incorporation.

DNA fragmentation after ionizing radiation, UV-A laser microbeam and chemical damage

Because IFCA is able to reveal subtle details about the fragmentation pattern, we looked at how this fragmentation pattern differs for different DNA DSB induction mechanisms at the single-cell level. Figure 3 shows typical comets after

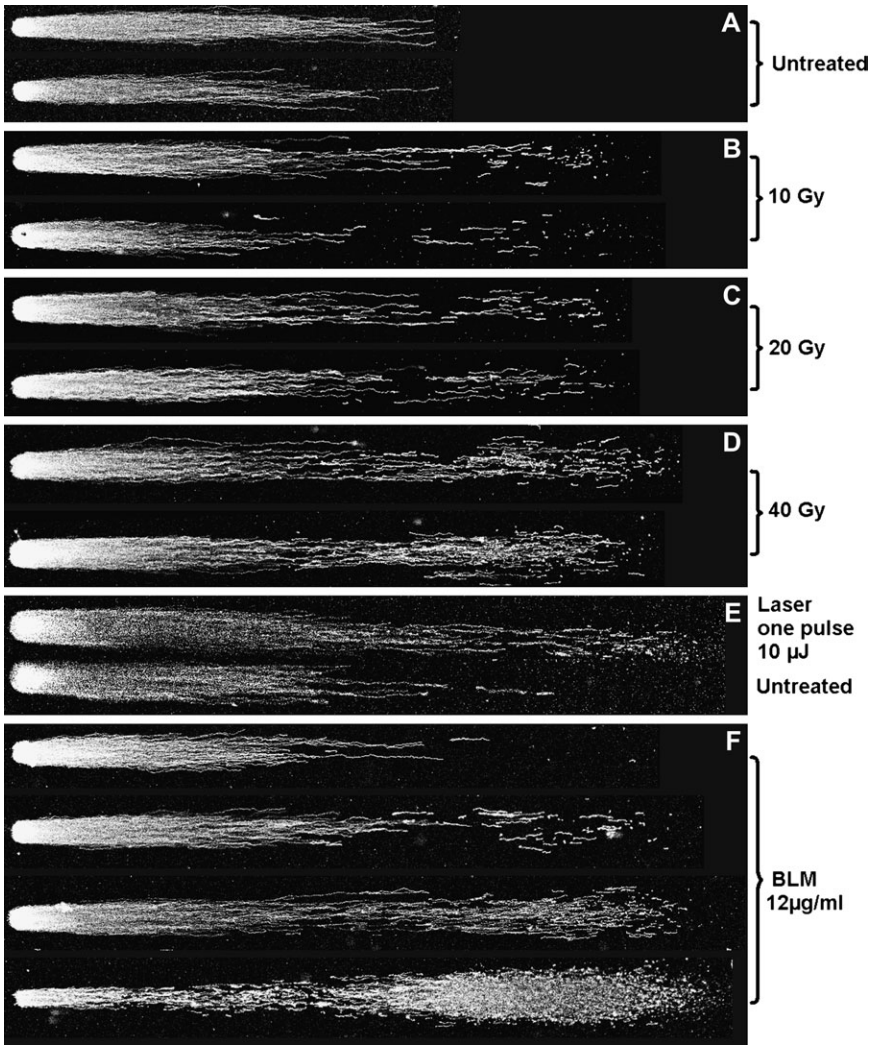

Fig. 3. Fragmentation patterns of differently damaged cells (IR, BLM, UV-A laser) after neutral lysis, 2-h electrophoresis and IFCA. The damage type and dose are given on the right-hand side. (**A**) Untreated cells do not show any fragmentation; (**B**, **C** and **D**) represent comets after exposure to 10, 20 and 40 Gy, respectively. (**E**) Top, comet after irradiation with one pulse of UV-A laser microbeam; bottom, untreated cell nearby. (**F**) Different fragmentation patterns after BLM treatment 12 μg/ml.

neutral IFCA of HeLa cells treated by ionizing radiation, UV-A laser microbeam irradiation and BLM.

In Figure 1, it was shown that untreated cells do not have fragments at the end of the tail. Indeed we do not see fragmentation even after 2 h of electrophoresis; all chromosomes appear to emanate out of the nucleus (Figure 3A). After 10-Gy irradiation, short fibre fragments as well as several dot-like fragments occur. The number of both short and dot-like fragments increases after irradiation with 20 and 40 Gy (Figure 3C and D).

In Figure 3E, DNA fragmentation after irradiation with one single 10 μJ (20 ns) pulse of a UV-A laser microbeam is shown in direct comparison with an untreated cell. Lasers induce a high number of small dot-like as well as short and longer fibre fragments (Figure 3E). From the intensity profiles in Figure 4, it is seen that the fragmentation pattern is similar to that after 20-Gy irradiation. The difference is only that damage after ionizing radiation is induced in the whole cell nucleus whereas damage after laser irradiation is induced in a small volume of laser focus. It shows that irradiation with a UV-A laser does induce a high concentration of SSBs and DSBs in a small volume of the cell nucleus, without an external sensitizer.

After the BLM treatment, the fragmentation level varies largely from cell to cell as was already reported by Ostling and Johanson (1). In Figure 3F, four different types of comets detected after 12 μg/ml BLM treatment are depicted. Similar comets can be found in untreated cells to those in cells with medium and very high fragmentation levels. It shows that DNA damage induction by BLM in asynchronous cells differs severely. It is possible that this variation is dependent on the cell cycle phase, where BLM uptake and the DNA access are different.

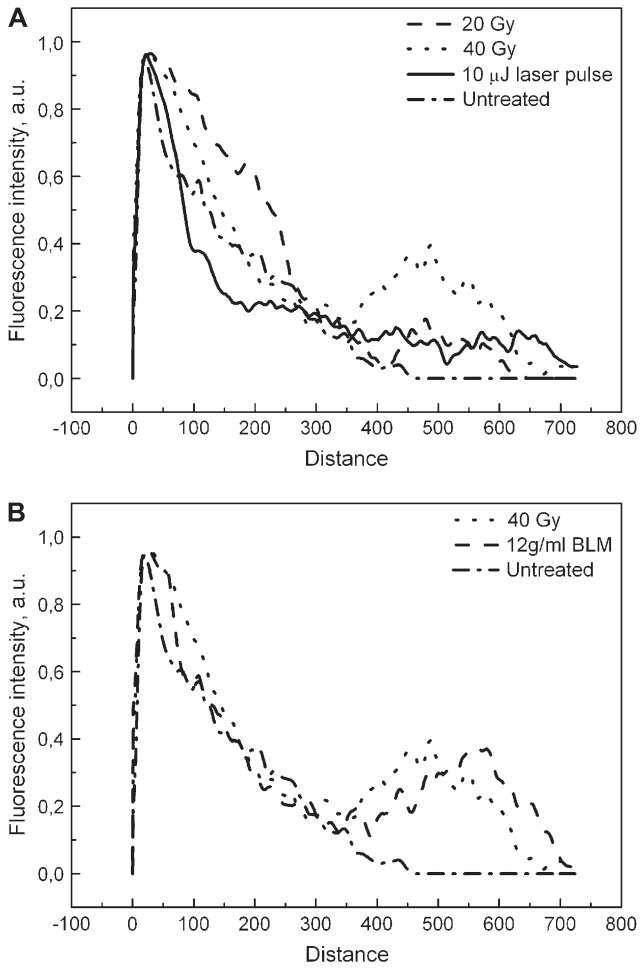

Fig. 4. (**A** and **B**) Comparison of intensity profiles showing that laser microirradiation-induced pattern is similar to the one induced by 20 Gy (**A**), when the third BLM comet has a pattern similar to that after 40 Gy (**B**).

Discussion

In the present study, we have established the neutral IFCA as a highly sensitive method with high resolution for the visualization of single-chromatin fibres and chromatin fragments. As a first result, we could show, by comparing the effects of nicking (SSB inducing) and cutting (DSB inducing) enzymes, that the neutral comet assay also detects a subclass of SSBs, which are induced in opposite DNA strands in close proximity (<14 nucleotides) and thus are finally converted to DSBs.

Furthermore, for the first time, we directly show the fragment size distribution in the neutral comet assay. From the lambda DNA migration pattern, we can assume that double-stranded fragments with the size of 48 kbp migrate 540 μm during 25 min of electrophoresis and are located at the end of the comet tail as dot-form structures. A similar result was predicted from the comparison of the *in silico* fragmentation analysis of cutting enzyme with its fragmentation pattern in the comet tail. This reveals that fragments up to 30 kbp are forming the dot-like fragments at the end of the tail.

Comparison of fragmentation patterns with different agents reveals that for BLM the damaging level differs from cell to cell (1). A treatment with 12 μg/ml BLM for 30 min results in a fragmentation pattern similar to that of 40 Gy ^{137}Cs exposure (Figure 4B). For this damage, millions of molecules in the whole cell nucleus are needed.

The DNA damage patterns after ionizing and UV-A radiation are surprisingly similar to each other. In particular, ionizing radiation of 20 Gy (photon energy 662 000 eV) induces a similar fragmentation pattern to that of 10 μJ laser irradiation (3.5 eV). It means that the photon number required to induce the same fragmentation pattern is $\sim 10^8$ times higher for UV-A laser treatment, although the energies of photons differ by only 2×10^5 times (Table I). Thus, the γ photons induce damage 500 times more efficiently than UV-A photons (350 nm), although the overall absorbed energy is the same (Table II).

The 500 times higher efficiency of γ irradiation compared to UV-A is probably due to physical and not biological effects. A significant difference in our irradiation protocol is that a small number of ionizing photons affects the whole cell nucleus. In contrast, the UV-A laser microbeam induces highly localized damage. Due to this, we delivered 10^{13} UV-A photons into the small volume of 3 μm^3 during a short-time period of 20 nsec. It means 10^6 photons/fsec—approximately one optical cycle. It

Table II. DNA fragmentation efficiency of treatments

Treatment	Number of photons or molecules	Relative break efficiency
20 Gy (^{137}Cs)	1.25×10^4	500
10 μJ UV-A, 350 nm laser pulse	1×10^{12}	1
BLM 12 μg/ml	1.5×10^6	n.a.

n.a. = not available.

probably causes the saturation of molecules in the excited state and many following photons cannot be absorbed. Consequently, the factor of 500 has to be taken as an empirical value and can be used for the comparison of UV-A and ionizing irradiation-induced effects in terms of DSBs.

Funding

Marie Curie Fellowship programme (MEIF-CT-2005-023821) to A.R.

Acknowledgements

We would like to thank Dr Shamci Monajembashi for support by building the laser microbeam irradiation set-up as well as Sabine Hoffmann, Gabi Günther and Silke Schulz for technical assistance with cell culture.

Conflict of interest statement: None declared.

References

1. Ostling, O. and Johanson, K. J. (1987) Bleomycin, in contrast to gamma-irradiation, induces extreme variation of DNA strand breakage from cell to cell. *Int. J. Radiat. Biol.*, **52**, 683–691.
2. Essers, J., Vermeulen, W. and Houtsmuller, A. B. (2006) DNA damage repair: anytime, anywhere? *Curr. Opin. Cell Biol.*, **18**, 240–246.
3. Bekker-Jensen, S., Lukas, C., Kitagawa, R., Melander, F., Kastan, M. B., Bartek, J. and Lukas, J. (2006) Spatial organization of the mammalian genome surveillance machinery in response to DNA strand breaks. *J. Cell Biol.*, **173**, 195–206.
4. Uematsu, N., Weterings, E., Yano, K. *et al.* (2007) Autophosphorylation of DNA-PKCS regulates its dynamics at DNA double-strand breaks. *J. Cell Biol.*, **177**, 219–229.
5. Greulich, K. O. (1999) *Micromanipulation by Light in Biology and Medicine—The Laser Microbeam and Optical Tweezers*. Birkhaeuser, Basel, Switzerland.
6. Berns, M. W. and Greulich, K. O. (2007) *Methods in Cell Biology: Laser Manipulation of Cells and Tissues*. Elsevier/Academic Press, New York.
7. Ward, J. F. (1988) DNA damage produced by ionizing-radiation in mammalian-cells—identities, mechanisms of formation, and reparability. *Prog. Nucleic Acid Res. Mol. Biol.*, **35**, 95–125.
8. Cullinan, E. B., Gawron, L. S., Rustum, Y. M. and Beerman, T. A. (1991) Extrachromosomal chromatin—novel target for bleomycin cleavage in cells and solid tumors. *Biochemistry*, **30**, 3055–3061.
9. Povirk, L. F., Wubker, W., Kohnlein, W. and Hutchinson, F. (1977) DNA double-strand breaks and alkali-labile bonds produced by bleomycin. *Nucleic Acids Res.*, **4**, 3573–3580.
10. Ostling, O. and Johanson, K. J. (1984) Microelectrophoretic study of radiation-induced DNA damages in individual mammalian cells. *Biochem. Biophys. Res. Commun.*, **123**, 291–298.
11. Olive, P. L., Wlodek, D., Durand, R. E. and Banath, J. P. (1992) Factors influencing DNA migration from individual cells subjected to gel electrophoresis. *Exp. Cell Res.*, **198**, 259–267.
12. Collins, A. R., Oscoz, A. A., Brunborg, G., Gaivao, I., Giovannelli, L., Kruszewski, M., Smith, C. C. and Stetina, R. (2008) The comet assay: topical issues. *Mutagenesis*, **23**, 143–151.
13. Singh, N. P., Stephens, R. E., Singh, H. and Lai, H. (1999) Visual quantification of DNA double-strand breaks in bacteria. *Mutat. Res.*, **429**, 159–168.
14. Werner, D. and Petzelt, C. (1981) Alkali-stably bound proteins in eukaryotic and prokaryotic DNAs show common characteristics. *J. Mol. Biol.*, **150**, 297–302.
15. Rapp, A., Hausmann, M. and Greulich, K. O. (2005) The comet-FISH technique: a tool for detection of specific DNA damage and repair. *Methods Mol. Biol.*, **291**, 107–119.
16. Grigaravicius, P., Monajembashi, S., Pilarczyk, G., Rapp, A. and Greulich, K. O. (2007) Laser microbeams and optical tweezers to study DNA repair and ageing. *Proc. Soc. Photo. Instrum. Eng.*, **6644**, .
17. Vispe, S. and Satoh, M. S. (2000) DNA repair patch-mediated double strand DNA break formation in human cells. *J. Biol. Chem.*, **275**, 27386–27392.
18. Gulston, M., Fulford, J., Jenner, T., de Lara, C. and O'Neill, P. (2002) Clustered DNA damage induced by radiation in human fibroblasts (HF19), hamster (V79-4) cells and plasmid DNA is revealed as Fpg and Nth sensitive sites. *Nucleic Acids Res.*, **30**, 3464–3472.

Received on August 4, 2008; revised on November 14, 2008; accepted on November 16, 2008